Mesoporous Titanium Phosphate Molecular Sieves with Ion-Exchange Capacity

Asim Bhaumik and Shinji Inagaki*

Contribution from the Toyota Central R & D Labs. Inc., Nagakute, Aichi 480-1192, Japan

Received July 7, 2000

Abstract: Novel open framework molecular sieves, titanium(IV) phosphates named, i.e., TCM-7 and -8 (Toyota Composite Materials, numbers 7 and 8), with new mesoporous cationic framework topologies obtained by using both cationic and anionic surfactants are reported. The ^{31}P MAS NMR, UV−visible absorption, and XANES data suggest the tetrahedral state of P and Ti, and stabilization of the tetrahedral state of Ti in TCM-7/8 is due to the incorporation of phosphorus (at Ti/P = 1:1) vis-à-vis the most stable octahedral state of Ti in the pure mesoporous TiO_2. Mesoporous TCM-7 and -8 show anion exchange capacity due to the framework phosphonium cation and cation exchange capacity due to defective P−OH groups. The high catalytic activity in the liquid-phase partial oxidation of cyclohexene with a dilute H_2O_2 oxidant supports the tetrahedral coordination of Ti in these materials.

Introduction

Aluminosilicate zeolites[1−3] with an anionic framework and cation exchange capacity have been extensively studied and used as acid catalysts, adsorbents, and ion exchangers in the chemical and petrochemical industries. Phosphate-based molecular sieves[4−6] with mostly a neutral framework have also attracted considerable attention of the academia and industry. Commercial anion exchangers are mostly organically based, such as anion-exchange resins. While cation-exchange materials are very common for inorganic materials (e.g. zeolites), anion-exchangeable inorganic materials are very rarely mentioned in the literature. Hydrotalcite[7] and mesoporous aluminophosphate derived from polyoxometalate clusters[8,9] are the only examples of such a class of materials. On the other hand, the development of light-driven photocatalysts has been urgent from the viewpoint of not only efficient decomposition of water[10,11] to produce hydrogen as an alternative energy source but also of reduction of the amount of carbon dioxide in the atmosphere, which is one of the most important problems in connection with the "greenhouse effect". The incorporation of Ti in the SiO_2 frameworks of micro- and mesoporous materials is also of outstanding interest because of their remarkable applicability to liquid-phase oxidation (at 1−3 wt % loading on silica[12]) reactions. However, the small pores of such highly active microporous titanium silicates[12] restrict their application to only smaller organic molecules (C_3−C_7).[13] Thus inorganic mesoporous materials with a framework Ti and zeolite-like ion-exchange properties are highly desirable.

Although there have been many reports on layered[14] and open-framework[15] titanium phosphates, there are very few reports on porous titanium phosphates.[16] Very recently, Jones et al.[17] reported the synthesis of mesoporous titanium phosphate using cationic surfactant and its surface acidity. Although the mesoporous titanium phosphate had a big potential to be used as a catalyst for liquid-phase oxidation reactions and photoreactions, little attention was paid to the coordination structure of Ti and catalysis of such reactions in the report. We have succeeded in the synthesis of mesoporous titanium phosphates, independently, by using not only cationic surfactants but also anionic surfactants. Here, we report a synthesis, detail structures, ion-exchange properties, and partial oxidation catalysis of the novel mesoporous titanium phosphates. We propose a model of Ti, P, and O connectivities in the framework of the mesoporous titanium phosphate on the basis of characterization results by ^{31}P MAS NMR, UV−visible absorption, XANES, IR, and water vapor adsorption measurements. And we show that the mesoporous titanium phosphates have unusually simultaneous cation and anion exchange capacities due to the defect P−OH groups and framework phosphonium cations, respectively. The ion-exchange properties of the mesoporous titanium

* Address correspondence to this author. E-mail: inagaki@mosk.tytlabs.co.jp. Fax: +81-561-63-6498.

(1) Barrer, R. M. *Hydrothermal Chemistry of Zeolites*; Academic Press: New York, 1982.
(2) Szostak, R. *Molecular Sieves: Principles of Synthesis and Identification*; Van Nostrand Reinhold: New York, 1989.
(3) Corma, A. *Chem. Rev.* **1997**, *97*, 2373−2419.
(4) Wilson, S. T.; Lok, M. M.; Messina, C. A.; Cannan, T. R.; Flanigen, E. M. *J. Am. Chem. Soc.* **1982**, *104*, 1146−1147.
(5) Davis, M. E.; Saldarriaga, C.; Montes, C.; Garces, J.; Crowder, C. *Nature* **1988**, *331*, 698−699.
(6) Serre, C.; Ferey, G. *J. Mater. Chem.* **1999**, *9*, 579−585.
(7) Matsushita, T.; Ebitani, K.; Kaneda, K. *Chem. Commun*. **1999**, 265−266.
(8) Holland, B. T.; Isbester, P. K.; Blanford, C. F.; Munson, E. J.; Stein, A. *J. Am. Chem. Soc.* **1997**, *119*, 6796−6803.
(9) Kron, D. A.; Holland, B. T.; Wipson, R.; Maleke, C.; Stein, A. *Langmuir* **1999**, *15*, 8300−8308.
(10) Anpo, M.; Yamashita, H.; Ichihashi, Y.; Fujii, Y.; Honda, M. *J. Phys. Chem. B* **1997**, *101*, 2632−2636.
(11) Domen, K.; Kudo, A.; Onishi, T. *J. Catal*. **1986**, *102*, 92−98.
(12) Notari, B. *Adv. Catal.* **1996**, *41*, 253.
(13) Venuto, P. B. *Microporous Mater.* **1994**, *2*, 297−400.
(14) Clearfield, A.; Costantino, U. *Comprehensive Supramolecular Chemistry*; Elsevier: Amsterdam, 1996; Vol. 7, pp 107−149.
(15) Ekambaram, S.; Sevov, S. C. *Angew. Chem., Int. Ed.* **1999**, *38*, 372−375.
(16) Thieme, M.; Schüth, T. *Microporous Mesoprous Mater*. **1999**, *29*, 193−200.
(17) Jones, D. J.; Aptel, G.; Brandhorst, M.; Jacquin, M.; Roziére, J.; Jiménez-Jiménez, J.; Jiménez-López, A.; Maireles-Torres, P.; Piwonski, I.; Rodríguez-Castellón, E.; Zajac, J.; Roziére, J. *J. Mater. Chem.* **2000**, *10*, 1957−1963.

10.1021/ja002481s CCC: $20.00
Published on Web 01/09/2001

phosphate are very useful for use as a catalyst, because reactants can be concentrated onto the surface of the catalyst.

Experimental Section

Starting Materials. Cationic surfactants, like octadecyltrimethylammonium chloride (ODTMACl) and octadecyltrimethylammonium bromide (ODTMABr), and anionic surfactants, like sodium dodecyl sulfate (SDS) and dodecyl *p*-benzenesulfonic acid (DBSA), were obtained from Tokyo Chemical Industries, and titanium isopropoxide, $TiCl_4$, H_3PO_4, $AgNO_3$, EtOH, HCl, NaOH, and liquid ammonia were purchased from Wako Chemicals.

Synthesis. Cationic surfactant octadecyltrimethylammonium halides (ODTMACl and ODTMABr for TCM-7 and -8, respectively) were found to be efficient structure directing agents (SDAs) for the synthesis of mesoporous titanium phosphates when titanium isopropoxide $Ti(OPr)_4$ was used as the Ti source. TCM-7 and -8 can also be synthesized efficiently in the presence of anionic surfactants, i.e., SDS (TCM-7) and DBSA (TCM-8), with $TiCl_4$ as the Ti source. In a typical synthesis with a cationic surfactant, ODTMABr/Cl was dissolved in water and the required amount of H_3PO_4 was added to it, and then the mixture was homogenized by vigorous stirring. Then $Ti(OPr)_4$ dissolved in an equal amount (wt/wt) of isopropyl alcohol was added slowly to the mixture. After 1 h of stirring, the pH of the solution was adjusted to ca. 4.0 with liquid ammonia. For anionic surfactants, first an SDA was dissolved along with the required H_3PO_4 in water, and then $TiCl_4$ was added to the mixture slowly. Finally the pH was adjusted to ca. 4.0 and additional H_2O was added. Then the resultant slurry was heated at 318−348 K for 1 day under autogenous pressure. For Me-TCM-7 (sample 2), equimolar concentrations of H_3PO_4 and methylphosphonic acid dimethyl ester were used as phosphorus sources. The molar gel ratio of the reactants was:

$$TiCl_4/Ti(OPr)_4{:}H_3PO_4{:}(0.25-0.5)SDA{:}130H_2O{:}(0.05-0.25)NH_4OH$$

For the synthesis of pure titania with a mesoscopic framework, i.e., TiO_2−SDS (sample 3) and TiO_2−DBSA (sample 6), SDS and DBSA were used as surfactants. In a typical synthesis of TiO_2−DBSA, 16.5 g of DBSA was dissolved in 150 mL of water and $TiCl_4$ (18.9 g) was added dropwise to it with constant stirring. After 1 h the pH of the solution was adjusted to ca. 4.0 with liquid ammonia and the resultant slurry was heated at an elevated temperature. After the synthesis, the product was filtered off, washed with water, and then dried under vacuum at room temperature. Surfactants were removed from the as-synthesized materials by HCl/EtOH (sample 1 synthesized with ODTMACl and sample 4 synthesized with ODTMABr) or NH_4OH/EtOH (sample 2 synthesized with SDS and sample 5 synthesized with DBSA) extraction for 4 h at 298 K. Typically, 2 g of as-synthesized material was treated with 2 mL of 2 mol % HCl or 2 mL of 25% aqueous NH_4OH in 150 mL of EtOH. The anion exchange capacity of these titanium phosphates was evaluated by potentiometric titration of the filtrates obtained on treatment of the Cl-forms of TCM-7/-8 samples with NH_4OH/H_2O. An aqueous $AgNO_3$ solution was used for the titration. Cation exchange capacities were measured by the acid−base titration and by chemical analysis of the exchanged solid.

Characterization. XRD patterns were obtained with a Rigaku RINT-2200 diffractometer with Cu−Kα radiation. Transmission electron micrographs (TEMs) were obtained with a JEOL JEM-200CX at an accelerating voltage of 200 kV. Scanning electron micrographs (SEMs) for various samples were obtained with a JEOL JSM-890. Nitrogen adsorption isotherms were obtained with a Quantachrome Autosorb-1 at 77 K. UV−visible diffuse reflectance spectra were obtained with a JASCO V-570 equipped with an integrating sphere. FT-IR spectra of as-synthesized and surfactant-free samples were recorded with a JASCO FT/IR-5M. For ^{31}P MAS NMR measurements, a Bruker MSL-300WB spectrometer was used at 121.49 MHz. The chemical shifts on ^{31}P NMR were referenced to H_3PO_4 at 0 ppm. Chemical analysis of various samples was carried out by ICP. X-ray absorption near-edge structures (XANES) were recorded with a Laboratory EXAFS (EXAC820, Technos) using a Ge (220) crystal monochromator in the transmittance mode at room temperature. The samples were evacuated at room temperature before measurement of the XANES spectra. Liquid-phase oxidation reactions were carried out in two-necked round-bottom flasks fitted with a condenser and placed in an oil bath at 333 K with vigorous stirring. Then the reaction products were analyzed by capillary GC (FID) and identified with known standards and GC-MS.

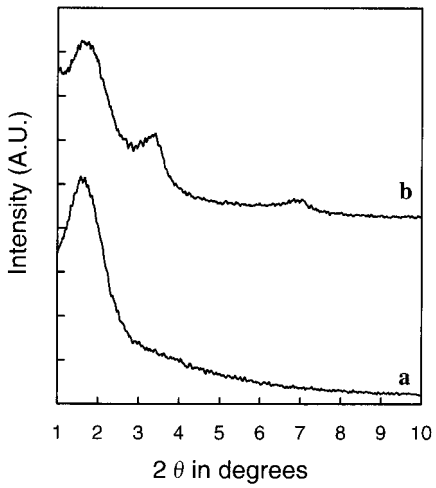

Figure 1. XRD patterns of the as-synthesized TCM-7 (a, sample 1) and TCM-8 (b, sample 4).

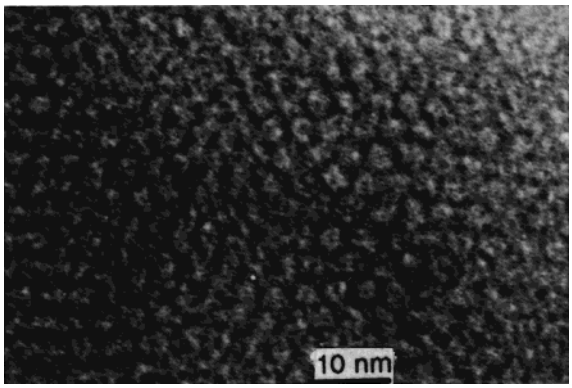

Figure 2. TEM image of as-synthesized Me-TCM-7 (sample 2).

Results and Discussion

From the XRD patterns the products were classified into two types of mesophases, TCM-7 and TCM-8. Typical XRD patterns of the as-synthesized TCM-7 (sample 1) and TCM-8 (sample 4) are shown in Figure 1. TCM-7 gave a single low-angle peak and no distinctive higher order peaks. TEM (Figure 2) showed that a portion of the hexagonal arrangement of uniform mesopores existed in the TCM-7 mesophase. These results suggest that TCM-7 has a poorly ordered two-dimensional hexagonal (*p*6*mm*) mesophase. The peak positions remained almost unchanged after removal of the surfactant, although the intensity decreased. TCM-8, on the other hand, showed some notable peaks in the low-angle region, suggesting the formation of another mesophase. It is important to note that the use of SDS as an SDA in the synthesis of TCM-7 along with $TiCl_4$ as the Ti source often leads to other lamellar mesophases at low temperature. This can be overcome by increasing the hydrothermal synthesis temperature. However, with DBSA as an SDA, no lamellar phase was observed. Chemical analysis of these titanium phosphates after the extraction revealed the absence of any organic SDA.

In Figure 3, N_2 adsorption/desorption isotherms for Me-TCM-7 (a, sample 2), TCM-7 (b, sample 1), and TCM-8 (c,

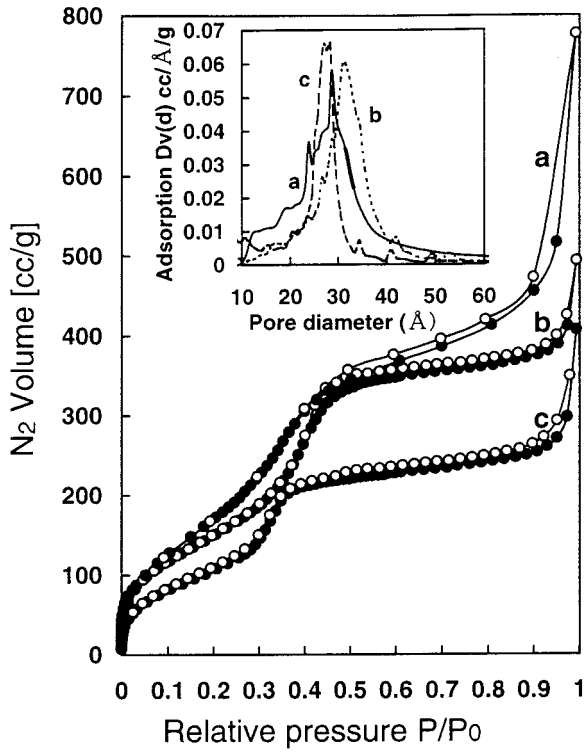

Figure 3. N_2 adsorption isotherms for Me-TCM-7 (a, sample 2), TCM-7 (b, sample 1), and TCM-8 (c, sample 4) at 77 K, recorded with an AUTOSORB-1, QUANTACHROME; pore size distributions (BJH) are shown in the inset. Adsorption points are indicated by filled circles and those of desorption by empty circles. Before the adsorption measurements all the samples were evacuated for 2 h at room temperature.

sample 4) are shown. These isotherms were type IV in nature.[18−21] The corresponding pore size distributions (Figure 3, inset) showed that these materials have narrow pore size distributions. The pore diameters, with the BJH model, and the BET surface areas of these samples are presented in Table 1. The pore diameters of the mesoporous titanium phosphates were 27.4−31.3 Å, which were almost comparable to those of mesoporous silicas prepared with the same surfactants. The BET surface areas of these mesoporous titanium phosphates were very high, e.g., as high as 701 $m^2\ g^{-1}$ for sample 2, this being the maximum. The pore walls were relatively thicker (42.8 Å and 29.0) for samples 1 and 2, respectively, than those of siliceous MCM-41 materials (15−22 Å).[18−21]

Since there were no noticeable high-angle reflections in the XRD patterns of these mesoporous titanium phosphates, the pore walls must be amorphous in nature. The TCM-7 and -8 samples exhibited unusually high anion-exchange capacities, 4.7−5.4 mmol g^{-1}, as listed in Table 1. These values are higher than those of other well-known anion exchangers, such as ion-exchange resins (1−4 mmol g^{-1}) and aluminophosphate mesoporous materials (1−4 mmol g^{-1}).[8,9] The anion-exchange capacities are almost equivalent to the contents of Ti and P atoms (5.6 mmol g^{-1}) in these materials. This suggests that the anion-exchange sites are generated in the framework due to the incorporation of Ti and P atoms.

^{31}P MAS NMR spectra of the titanium phosphate samples showed a broad signal with chemical shifts between 10 and −25 ppm. The TCM-7-ODTMACl materials before/after extraction of the surfactant gave intense peaks with chemical shifts of −4.5 and −5.0 ppm, respectively (Figure 4). An additional peak at 40 ppm was observed for the Me-TCM-7-SDS material, which was assigned as phosphorus attached to a methyl group. The TCM-8 materials also showed broad peaks with chemical shifts of −1.8 (sample 5) and −5.1 ppm (sample 4). These peaks can be assigned to a mixture of tetrahedral P environments with connectivity 3 and 4 [$(P(OTi)_3OH$ and $P(OTi)_4$], respectively. Mesostructured $AlPO_4$ materials show signals between −1.4 and −1.9 ppm due to PO_4 tetrahedras.[22] Tetrahedral phosphorus in the neutral microporous aluminophosphate materials shows a strong sharp band at around −28 to 30 ppm[23] (with respect to H_3PO_4) in the ^{31}P MAS NMR spectra. Due to the lack of resolution the relative concentrations were unobtainable from these spectra. Although the change in chemical shift during removal of the surfactant was small (0.5 ppm) for TCM-7-ODTMACl (sample 1), it was large (8.8 ppm, from −9.8 to −1.0 ppm) for Me-TCM-7-SDS (sample 2). This large change in the chemical shift is attributable to the direct interaction between the phosphonium cations (P^+) and anions (SDS^- or OH^-) for the Me-TCM-7-SDS system but indirect interaction between $P-O^-$ and cations ($ODTMA^+$ or H^+) for the TCM-7-ODTMACl system.

The UV−visible spectra of the titanium phosphate materials showed a very strong absorption band in the 220−330 nm wavelength region (Figure 5, curves a and b, due to the electronic transition from O^{2-} 2p to Ti^{4+} 3d orbitals). The mesoporous TiO_2 samples synthesized with SDS (sample 3) and DBSA (sample 6, Figure 5) in the absence of H_3PO_4 show an absorption edge at 390 nm. This band is similar to that of anatase titania and can be attributed to the octahedral coordination of Ti in the TiO_2 network. A similar high-energy absorption edge due to tetrahedral coordination of Ti has been observed for mesoporous titanosilicate (300−330 nm),[24] Ti-exchanged Y-zeolite (320 nm),[10] and Ti-containing amorphous silica (325−350 nm).[25] The high-energy absorption band of titanium phosphates indicates that the tetrahedral coordination of Ti is dominant in these materials. Microporous titanium silicate TS-1, with tetrahedral Ti, gives a strong absorption band at 200−220 nm. This high-energy absorption band is attributable to the low content of Ti (2−2.2 mol %) of TS-1, the titanium phosphates studied here having a high content of Ti (32 mol %). An increase in Ti loading always leads to a considerable shift of UV−vis absorption to a higher wavelength.[25] The local environment of Ti also plays a crucial role in the shift of the absorption band. The environment with four −O−P attached to Ti in TCM-7/-8 instead of four −O−Si in TS-1 may be responsible for this shift. The local structure of Ti in these mesoporous titanium phosphate materials was obtained from the Ti K-edge XANES spectra, as shown in Figure 6. It is well-known that TiO_2 (both anatase and rutile) exhibits three weak preedge peaks in XANES spectra (corresponding to the transition of electrons from 1s to $^1t_{1g}$, $^2t_{2g}$, and ^3e_g orbitals), which are assigned to octahedral Ti.[10] On the other hand, the tetrahedrally coordinated Ti in a Ti-exchanged Y-zeolite[10] shows

(18) Huo, Q.; Margolese, D. I.; Stucky, G. D. *Chem. Mater*. **1996**, *8*, 1147−1160.
(19) Antonelli, D. M.; Ying, J. Y. *Angew. Chem., Int. Ed.* **1995**, *34*, 2014−2017.
(20) Kresge, C. T.; Leonowicz Roth, W. J.; Vartuli, J. C.; Beck, J. S. *Nature* **1992**, *359*, 710−712.
(21) Yang, P.; Zhao, D.; Margolese, D. I.; Chmelka, B. F.; Stucky, G. D. *Nature* **1998**, *396*, 152−155.
(22) Sayari, A.; Moudrakovski, I.; Reddy, J. S. *Chem. Mater*. **1996**, *8*, 2080−2088.
(23) Blackwell, C. S.; Patton, R. L. *J. Phys. Chem*. **1984**, *88*, 6135−6139.
(24) Zhang, W.; FrÖba, M.; Wang, J.; Tenev, P. T.; Wong, J.; Pinnavaia, T. J. *J. Am. Chem. Soc.* **1996**, *118*, 9164−9171.
(25) Kosuge, K.; Sing, P. S. *J. Phys. Chem*. **1999**, *103*, 3563−3569.

Table 1. Physicochemical Properties of Various Mesoporous Titanium Phosphates

sample no.	sample name-SDA[a]	Ti/P,[b] molar ratio	BET surface area, m^2g^{-1}	pore diameter, Å	anion exchange capacity, mmol g^{-1}
1	TCM-7-ODTMACl	1.02	548	31.3	5.41
2	Me-TCM-7-SDS	1.05	701	28.7	5.28
3	TiO_2−SDS	∝	550	21.8	
4	TCM-8-ODTBABr	1.03	420	27.4	4.80
5	TCM-8-DBSA	1.01	407	29.0	4.72
6	TiO_2-DBSA	∝	325	29.5	

[a] The structure directing agent (SDA) corresponding to each sample is indicated after the sample name. [b] As measured by ICP chemical analysis.

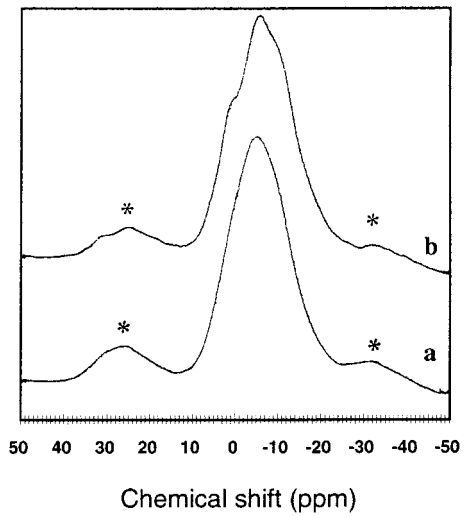

Figure 4. ^{31}P MAS NMR spectra of TCM-7 (sample 1): as-synthesized (a) and after surfactant removal (b), recorded with a BRUKER MSL 300. Spinning sidebands which appeared corresponding to multiples of the spinning rate are indicated by asterisks.

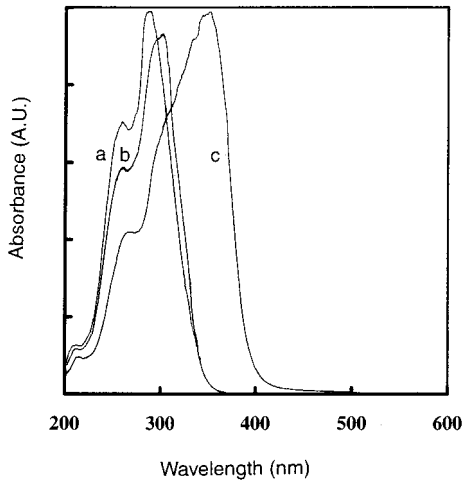

Figure 5. UV−visible diffuse reflectance spectra of samples 1 (a), 2 (b), and 6 (c) recorded with a JASCO V-570 equipped with an integrating sphere.

a single, intense preedge peak.[24−26] As shown in Figure 6, a single preedge peak was observed for TCM-7 (sample 1, Figure 6a), while some small preedge peaks were observed for anatase TiO_2 (Figure 6b). The low resolution of the spectra is attributable to the use of a Laboratory EXAFS instead of a Synchroton EXAFS instrument. These results indicate the presence of tetrahedrally coordinated Ti in the mesoporous titanium phosphates. However, the lower intensity of the preedge peak of TCM-7 than in the case of Ti-exchanged Y-zeolite suggests the presence of a partial Ti with 5- or 6-fold coordination in the

(26) Liu, Z.; Davis, R. J. *J. Phys. Chem.* **1994**, *98*, 1253−1259.

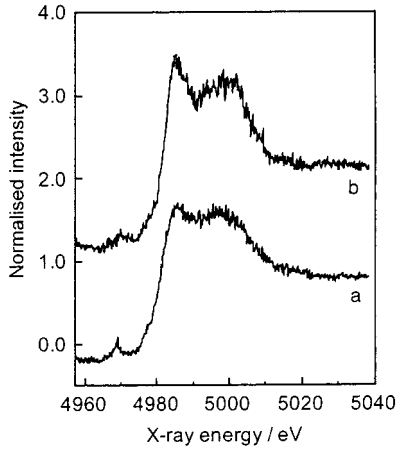

Figure 6. Ti K edge XANES spectra of TCM-7 (sample 1, a) and TiO_2 (anatase, b). Before the measurements, the samples were evacuated at room temperature for 3 h.

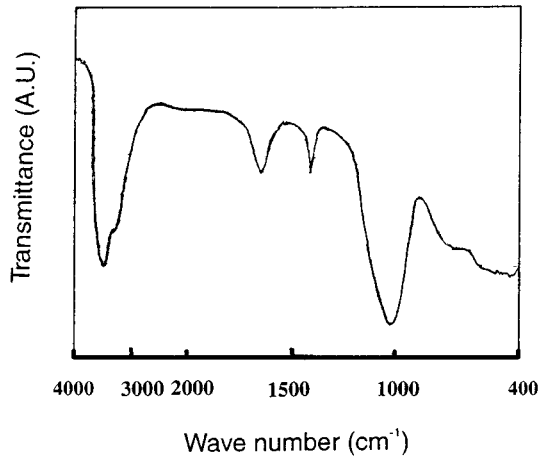

Figure 7. FT-IR spectra of TCM-7 (sample 1) after surfactant removal.

sample. These Ti species are attributable to the extraframework TiO_2. However, no peak corresponding to TiO_2 (anatase/rutile with octahedral Ti) was observed in the XRD patterns of these titanium phosphate materials.

In Figure 7, an FT-IR spectrum of TCM-7 (sample 1 being taken as representative) after surfactant removal is shown. Broad bands in the hydroxyl region with maximum at 3400 cm^{-1} were observed. This corresponds to a O−H stretching vibration of the residual water, exchangeable OH^-, and defective OH. The Ti−O−P framework vibrations, which appear at 1000−1050 cm^{-1}, become broad after surfactant removal. This band was absent for the mesoporous TiO_2 (samples 3 and 6) which is free of phosphorus, suggesting a Ti−O−P network in the mesoporous titanium phosphates.

Along with the anion exchange property, a cation exchange property was observed for TCM-7/-8 due to the defective P−OH groups. Unlike in silanols (Si−OH), in which O−H bonding is

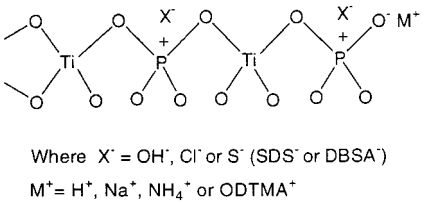

Figure 8. Proposed framework structure of titanium phosphates.

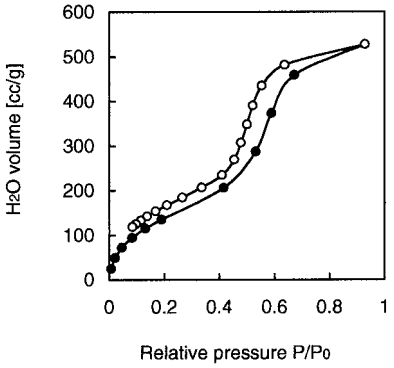

Figure 9. H_2O adsorption isotherm for TCM-7 (sample 1) at 298 K recorded with a BELSORP 18. Before the measurement, the sample was evacuated for 3 h at room temperature.

purely covalent, the high ionic character of the O−H bond in the $P-O^-H^+$ is responsible for this cation exchange capacity. The Cl-forms of various samples were treated with a known added amount of aqueous NaOH for 4 h at 298 K followed by titration of the filtrate with a standard oxalic acid solution to determine how much NaOH was consumed during the exchange process. The consumed NaOH amounted to 8.9 and 7.0 mmol g^{-1} for TCM-7 (sample 1) and Me-TCM-7 (sample 2), which were larger than the anion-exchange capacities, 5.4 and 5.3 mmol g^{-1}, respectively, determined with the $AgNO_3$ titration method. NaOH was consumed not only for exchange from Cl^- to OH^- on the P^+ site but also for exchange from H^+ to Na^+ at the defective $P-O^-$ site. So, the cation-exchange capacities were estimated to be 3.4 and 1.7 mmol g^{-1} for samples 1 and 2, respectively.

We propose a model for the Ti, P, and O connectivities in the framework of the titanium phosphate mesoporous materials based on the above results, as shown in Figure 8. Ti and P have regular alternating tetrahedral arrangements. This model explains the anion and cation exchange capacities of these materials. Both cationic and anionic surfactants can form this framework structure. Whereas in the cases of the use of anionic surfactants an I^+S^- (where I = inorganic framework and S = surfactant) assembly explains the mechanism of formation of the mesoporous titanium phosphate materials, I^-S^+ and $I^+X^-S^+$ miceller assemblies[19] can explain those with cationic surfactants.

H_2O vapor adsorption/desorption isotherms for sample 1 (taken as a representative) are shown in Figure 9. A type IV isotherm corresponding to great capillary condensation for the mesophase and hysteresis together with a great level of water vapor absorption at low P/P_0 was observed. The low-pressure adsorption of water vapor indicates strong interaction between the water and the solid surface. Such a high level of H_2O adsorption at low P/P_0 has been observed for Al-rich aluminosilicates[27] and this adsorption was attributed to the very strong adsorption of water at the Al sites, the level of adsorption linearly increasing with the number of framework Al[28] atoms per unit cell. For pure silica mesoporous materials,[29,30] a type V isotherm with very little H_2O adsorption of water at low P/P_0 was observed in the first adsorption/desorption cycle, indicating a very weak interaction between the H_2O and the surface. The great level of water adsorption at low P/P_0 suggests the generation of a charge and exchangeable sites for the 1:1 correspondence of Ti and P in these mesoporous titanium phosphate materials.

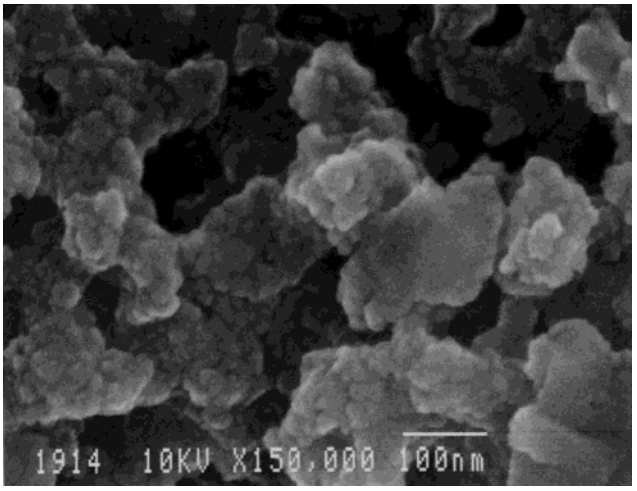

Figure 10. FE-SEM photograph of the as-synthesized TCM-8 (sample 4).

In general such titanium phosphate materials are stable up to 573 K. In the thermogravimetric weight loss (TG) and corresponding differential thermal analysis (DTA) curves, an endothermic peak in the temperature range of 298−423 K was observed. This is attributed to the loss of water molecules, i.e., a 12.5% weight loss. Next, the broad exothermic peak (33.8% weight loss) in the temperature range 493−693 K corresponds to thermal cracking and oxidative decomposition of the template as well as collapse of the framework.

SEM photographs of TCM-7 and -8 (Figure 10) showed that very small cubic to spherical crystals 20−60 nm in size form large spherical aggregates of 0.1 to 0.2 μm. The particle sizes of these titanium phosphate materials are quite small and uniform, unlike in the case of mesoporous silicas. Mesoporous materials with a very small particle size have been in great demand since their discovery[20] as this is an essential criterion for an efficient catalyst. Titanium silicates, specially TS-1,[12] have been extensively studied in a variety of organic reactions involving dilute hydrogen peroxide. The presence of a tetrahedral framework Ti, hydrophobicity, and a small particle size (i.e., a relatively high external surface area-to-volume ratio and reduced mass transfer resistance) are prerequisite for such efficient liquid-phase oxidation catalysts. Me-TCM-7 (sample 2) was used (chosen because of its relatively high surface area and relative hydrophobicity) for the liquid-phase oxidation of cyclohexene with a dilute H_2O_2 (25% aqueous) oxidant under mild conditions (333 K). In a typical reaction (substrate: H_2O_2 = 1:1, 8 h reaction time, solvent acetone) 76 mol % of cyclohexene was converted into 1,2-cyclohexanediol (dihydroxylation product, with 88% selectivity) and 2-cyclohexene-

(27) Wang, Z. B.; Ikeya, H.; Sano, T.; Soga, K. In *Proceedings of 12th International Zeolite Conference*; Treacy, M. M. J., Marcus, B. K., Bisher, M. E.,Higgins, J. B., Eds.; Materials Research Society: Baltimore, 1998; Vol. I, pp 293−300.

(28) Sano, T.; Fukuta, S.; Wang, Z. B.; Soga, K. In *Proceedings of 12th International Zeolite Conference*; Treacy, M. M. J., Marcus, B. K., Bisher, M. E., Higgins, J. B., Eds.; Materials Research Society: Baltimore, 1998; Vol. I, pp 301−307.

(29) Ribeiro Carrott, M. M. L.; Estevao Candeias, A. J.; Carrott, P. J. M.; Unger, K. K. *Langmuir* **1999**, *15*, 8895−8901.

(30) Inagaki, S.; Fukushima, Y. *Microporous Mesoporous Mater.* **1998**, *21*, 667−672.

1-ol (allylic oxidation product, with 12% selectivity). The catalytically active site for such liquid-phase oxidation reactions in the presence of dilute H_2O_2 is the tetrahedral Ti,[12] which generates the titanium hydroperoxo[31] species in situ. This titanium hydroperoxo species in turn oxidizes the olefin to the corresponding epoxide. The formation of 1,2-cyclohexanediol, which was observed as a major product under the present reaction conditions, can be attributed to the acid-/base-catalyzed hydrolysis of the cyclohexene oxide generated at the initial stage. This high catalytic activity of Me-TCM-7 in the liquid-phase oxidation reaction in the presence of H_2O_2 as an oxidant also suggests that the tetrahedral nature of Ti in these titanium phosphate materials, as molecular sieves containing octahedral Ti (e.g., ETS-10,[32] etc.), is completely inactive for such reactions. The energy gaps in the mesoporous titanium phosphates were estimated to be ca. 3.8 eV from the adsorption edge (330 nm) in the UV−vis spectrum, which was larger than that of TiO_2 (ca. 3.0 eV). The UV-light absorption property of these titanium phosphate molecular sieves together with the very large surface area and ion-exchange property is expected to allow their utilization as photocatalysts, such as in H_2 evolution[33,34] from water. The uniform pores along with the large internal surface area of these materials should make them accessible to water molecules, and the highly charged structure (1:1 correspondence of Ti and P) existing on the surface of a catalyst should facilitate the charge separation process essential for the photodecomposition of water. A detailed study on the photocatalytic behavior of these novel titanium phosphates is underway and the results will be published soon.

(31) Bhaumik, A.; Tatsumi, T. *J. Catal.* **1999**, *182*, 349−356.
(32) Anderson, M. W.; Terasaki, O.; Oshuna, T.; Philippou, A.; MacKay, S. P.; Ferreira, A.; Rocha, J.; Lidin, S. *Nature* **1994**, *367*, 347−351.
(33) Sayama, K.; Arakawa, H. *J. Chem. Soc., Faraday Trans. 1* **1997**, *93*, 1647−1654.
(34) Kudo, A.; Sekizawa, M. *Catal. Lett.* **1999**, *58*, 241−243.

Conclusion

Mesoporous titanium phosphates can be synthesized by using both cationic and anionic surfactants as SDAs. While $TiCl_4$ is a suitable Ti source for anionic surfactants, Ti-alkoxide is the most suitable for the synthesis of these titanium phosphates in the presence of cationic surfactants. UV absorption and XANES studies revealed that most of the Ti in these titanium phosphate materials is tetrahedrally coordinated. These mesoporous titanium phosphate materials have a very high surface area accessible through alternate regular coordination of TiO_4 and PO_4 tetrahedras. These novel materials have very high anion exchange capacities coupled with moderately high cation exchange capacities. These materials will be good liquid-phase oxidation catalysts. The novel methodology reported here for the synthesis of ordered mesoporous titanium phosphates materials will have many potential uses, e.g., in the production of ion exchangers, acid−base catalysts, photocatalysts, liquid-phase oxidation catalysts, etc.

Acknowledgment. We wish to thank Mr. N. Suzuki and Mr. H. Kadoura for their help in the TEM and FE-SEM measurements, respectively. We would also like to thank Prof. K. Domen, Tokyo Institute of Technology, for the helpful discussions and Dr. H. Yoshida, Nagoya University, for the measurement and discussion of the XANES spectra.

JA002481S